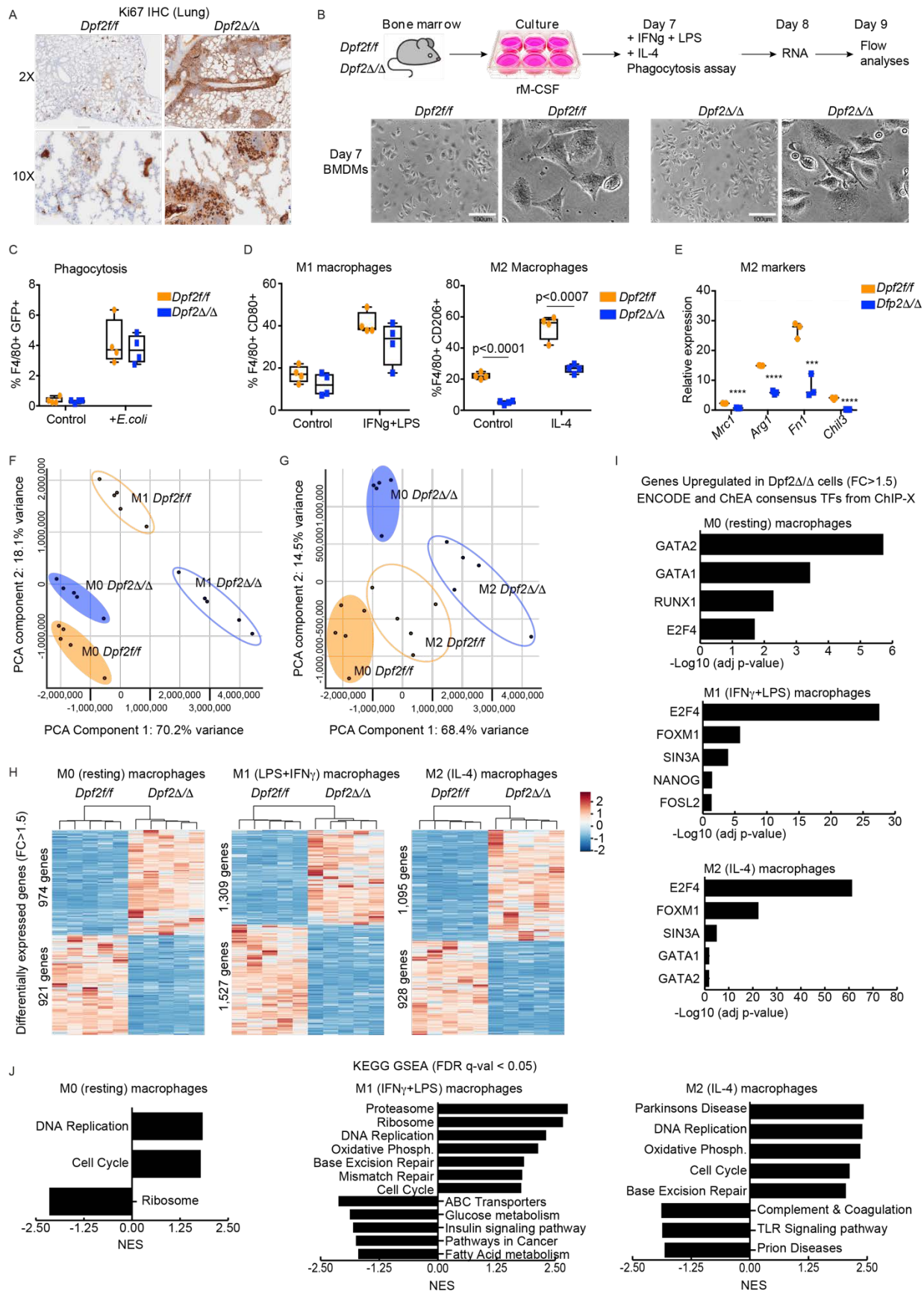


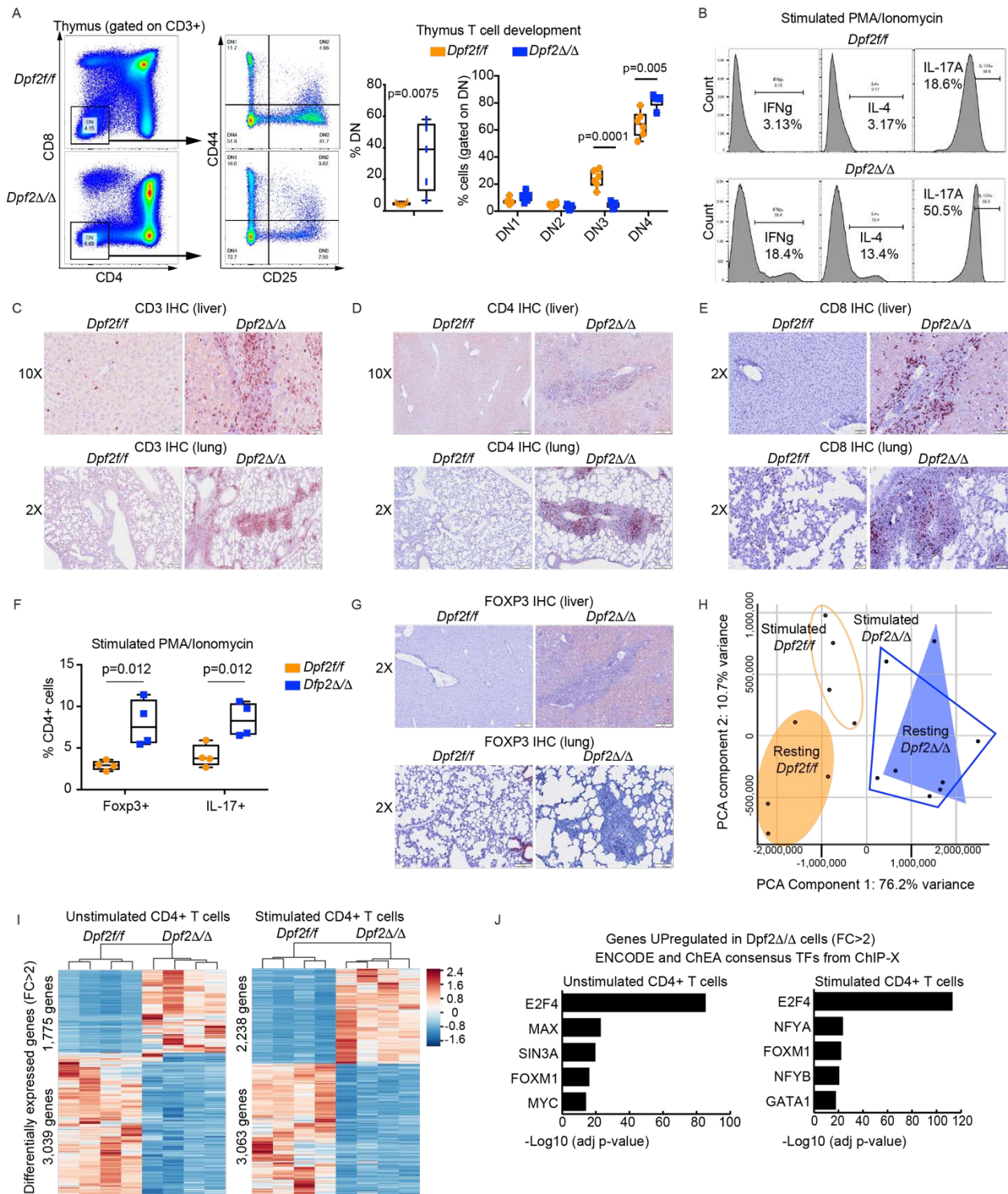
### Supplementary Figure 1. Inflammatory infiltrates and impaired survival in *Dpf2<sup>ΔΔ</sup>* mice

(A) Kaplan-Meier survival curves of the indicated groups of *Mx1-Cre* derived mice after Poly(I:C) administration (N=12-20 per genotype). (B) Relative *Dpf2* mRNA expression in PB, 2 weeks after Poly(I:C) administration. (C) PB CBC, 2 weeks after Poly(I:C) administration (N = 8). White blood cells (WBC), red blood cells (RBC). (D) Representative H&E images showing histiocytic infiltrations in liver and lung of mice analyzed 300 days after treatment with Poly (I:C). Scale bars represent 200  $\mu\text{m}$  (20X). (E) Representative CD68 IHC images of lung and liver, 300 days after Poly (I:C). (F) Same as (E), for CD69 IHC. Scale bars represent 50  $\mu\text{m}$ . (G) *Dpf2* mRNA expression levels in PB from *Vav1-Cre* crossed, 28 days old wild-type (*Dpf2<sup>fl/fl</sup>*), heterozygous (*Dpf2<sup>+Δ</sup>*) and *Dpf2* knock-out (*Dpf2<sup>ΔΔ</sup>*) mice. Western blot analysis of the indicated BAF subunits in BM Lin- cells. (H) Liver and spleen weight of 28-day-old mice. (I) Representative images of BM H&E staining. Scale bars represent 50  $\mu\text{m}$  (40X). (J) Wright-Giemsa stains of representative PB smears. Numbers indicate abnormal shape or size (anisocyte; 1), and Howell-Jolly bodies (2). Scale bars correspond to 50  $\mu\text{m}$ . (K) Galectin3/MAC2 IHC staining of BM and liver sections. Scale bars represent 20  $\mu\text{m}$  (for BM) and 200  $\mu\text{m}$  (for liver). (L) Reticulin staining of BM and liver sections. Scale bars represent 50  $\mu\text{m}$  (10X). All bar graph data represent mean  $\pm$  s.e.m.. *P*-values were calculated using two-tail unpaired Student's t-tests, except in Figure S1G where *p*-values were calculated using ordinary one-way ANOVA. Absence of *p*-value indicates no significant difference.



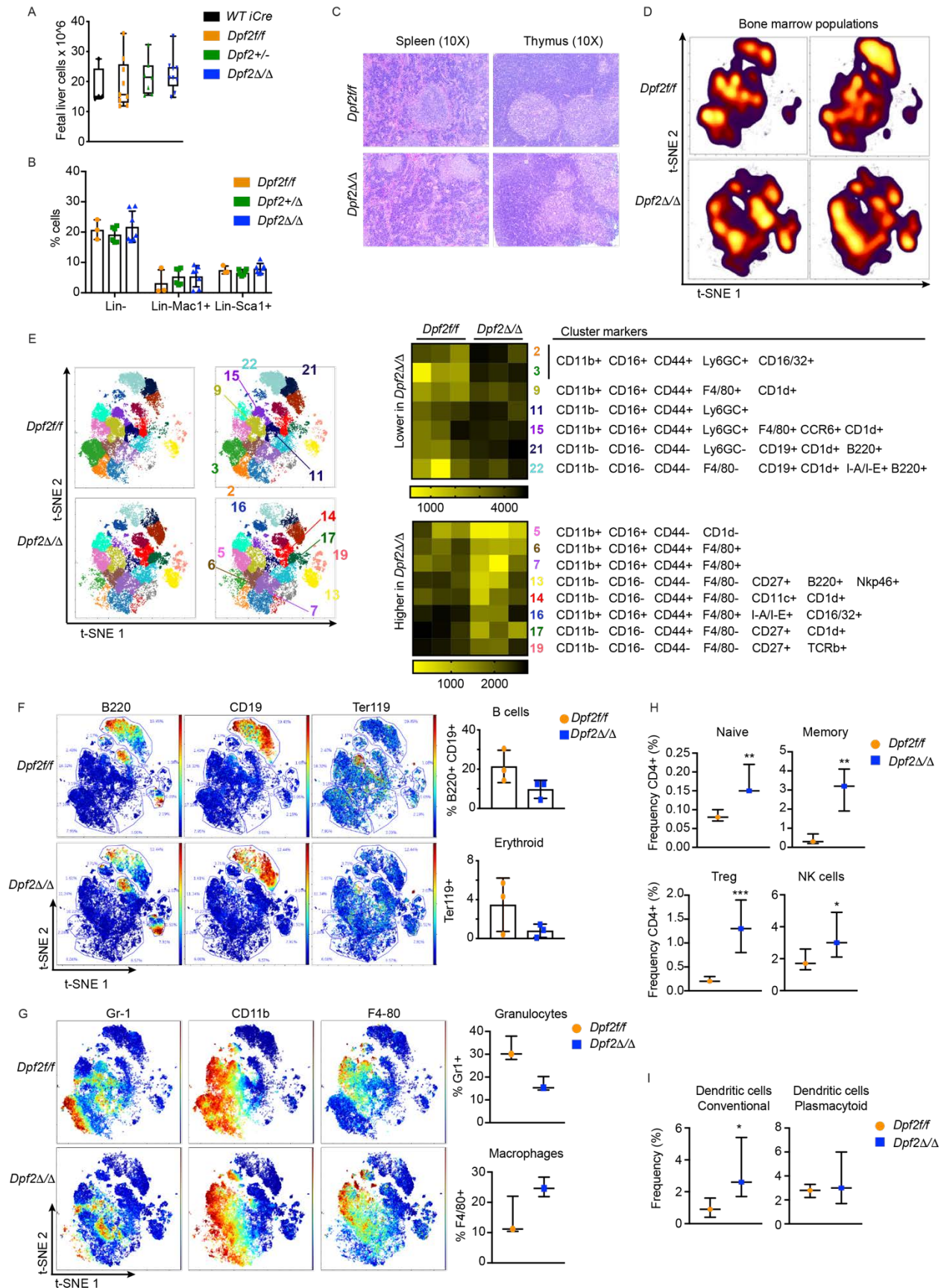
**Supplementary Figure 2. *Dpf2<sup>ΔΔ</sup>* macrophages show major transcriptional, proliferative and metabolic alterations associated with impaired immune activation.**

**(A)** Representative images of Ki67 IHC staining of lung sections, taken at 2X and 10X. **(B)** Experimental strategy to obtain BMDMs, and representative pictures of day 7 BMDMs. Scale bars represent 100  $\mu$ m. **(C)** Phagocytosis analysis of day 7 BMDMs treated with PBS (control) or GFP+ *E.coli*. **(D)** Frequency of BMDMs (F4/80+) untreated (control) or treated with IFN $\gamma$  plus LPS (M1 macrophages; CD80+) or with IL-4 (M2 macrophages; CD206+) for 48 hours. **(E)** qRT-PCR analysis of M2-specific markers in BMDMs treated for 24 hours with IL-4. **(F)** Principal Component Analysis (PCA) of RNA-Seq datasets from resting (M0) and M1 BMDMs, based on normalized expression counts. **(G)** Same as (F), for resting (M0) and M2 BMDMs. **(H)** Heatmaps of differentially expressed genes ( $q < 0.05$ ; fold change  $> 1.5$ ) between *Dpf2<sup>ΔΔ</sup>* and *Dpf2<sup>fl/fl</sup>* BMDMs (N=5; 28 days old) in resting conditions (M0), or after 24 hours of treatment. **(I)** ENCODE and ChEA consensus TFs from ChIP-X analysis obtained from the genes upregulated ( $q < 0.05$ ; fold change  $> 1.5$ ) in *Dpf2<sup>ΔΔ</sup>* compared to *Dpf2<sup>fl/fl</sup>* BMDMs in the indicated conditions. **(J)** GSEA KEGG analysis of gene expression programs enriched in *Dpf2<sup>ΔΔ</sup>* BMDMs in resting conditions (M0) or treated for 24 hours. All bar graph data represent mean  $\pm$  s.e.m. P values were calculated using two-tail unpaired Student's t-tests.



**Supplementary Figure 3. *Dpf2<sup>Δ/Δ</sup>* T cells are found in inflammatory lesions and display altered gene expression consistent with hyperproliferation and activation.**

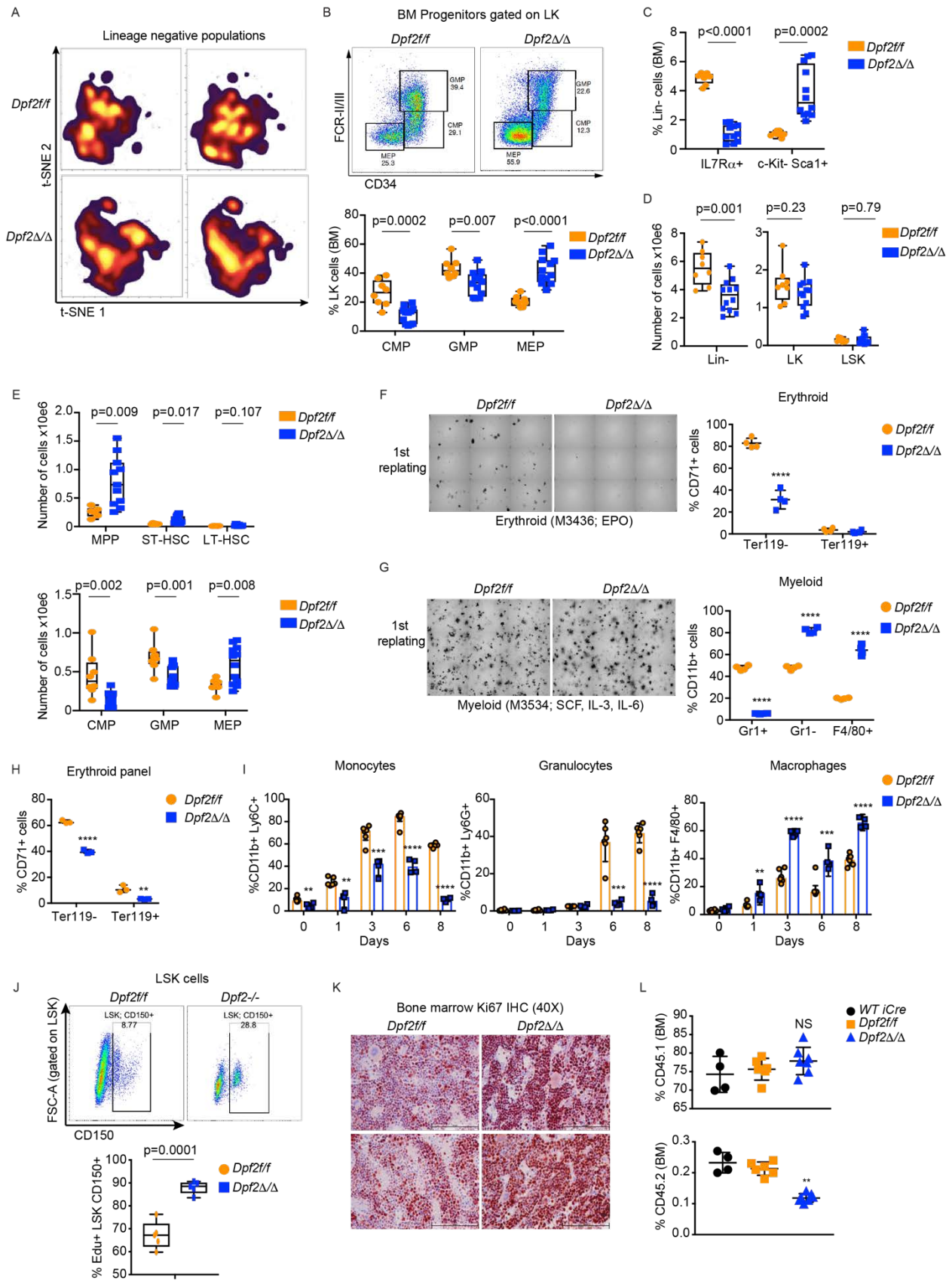
**(A)** Representative FACS of thymic CD3<sup>+</sup> T cell populations and analysis of Thymic T cell development. DN, Double Negative. **(B)** FACS profiles of splenic sorted CD4<sup>+</sup> T cell subsets stimulated with PMA/Ionomycin for 5 hours. Th1, Th2 and Th17 selectively secrete IFN $\gamma$ , IL-4 and IL-17a, respectively. **(C-E)** Representative images of CD3<sup>+</sup> (C), CD4<sup>+</sup> (D) and CD8<sup>+</sup> (E) IHC staining of liver and lung infiltrations. Scale bars represent 50  $\mu$ m (for CD3 and CD8) and 200  $\mu$ m (for CD4). **(F)** Flow cytometry analysis of intracellular cytokines expressed by sorted CD4<sup>+</sup> T cell subsets after ex vivo treatment with PMA and Ionomycin for 5 hours. Treg express FOXP3 and Th17 express IL-17. **(G)** Representative images of FOXP3 IHC staining in liver and lung. Scale bars represent 200  $\mu$ m. **(H)** PCA of normalized expression counts from RNA-Seq datasets obtained from resting and stimulated CD4<sup>+</sup> T cells. **(I)** Heatmaps of differentially expressed genes ( $q < 0.05$ ; fold change  $> 2$ ) between *Dpf2* <sup>$\Delta\Delta$</sup>  and *Dpf2*<sup>*fl/fl*</sup> splenic CD4<sup>+</sup> T cells (N=4; 28 days old mice) in resting or stimulated conditions. **(J)** ENCODE and ChEA consensus transcription factors from ChIP-X analysis obtained from the genes upregulated ( $q < 0.05$ ; fold change  $> 2$ ) in *Dpf2* <sup>$\Delta\Delta$</sup>  splenic CD4<sup>+</sup> T cells in the indicated conditions. All bar graph data represent mean  $\pm$  s.e.m. *P* values were calculated using two-tail unpaired Student's t-tests.



**Supplementary Figure 4. Early expansion of immature myeloid and T cell populations in *Dpf2<sup>ΔΔ</sup>* mice.**

**(A)** Absolute number of fetal liver cells in embryos of the indicated genotypes. **(B)** Frequency of the indicated fetal liver cell populations. **(C)** Representative H&E images of spleen and thymus of 14 days-old mice. Scale bars represent 50  $\mu\text{m}$  (10X). **(D)** viSNE analysis on all single, Ir+ Rh- cells from BM samples (28,390 events/sample) obtained from 14-day old *Dpf2<sup>ff</sup>* (top) and *Dpf2<sup>ΔΔ</sup>* (bottom) mice using all markers except Rho, c-CASP3, FOXP3. Cells were arranged along X and Y axes based on the similarity of their 29-dimensional phenotypes (Supplementary Table 2). Shaded contour plots depict cellular abundance ranging from purple (low) to yellow (high). **(E)** On the same viSNE axes as in (D), identification of cell clusters by the FlowSOM algorithm, using equal sampling on all single, Ir+ Rh- cells (28,390 events/sample). Each dot represents a cell. Numbers point to specific cell clusters that are downregulated (top) or upregulated (bottom) in *Dpf2<sup>ΔΔ</sup>* mice compared to *Dpf2<sup>ff</sup>*. Heatmaps show log<sub>2</sub> ratios of event counts by the minimum value between all 3 samples using X-axis channel(s). Markers of each cell cluster are indicated on the right. **(F)** On the same viSNE axes, expression levels of B cell markers (B220; CD19) and the erythroid marker Ter119 in all cells that are positive for each marker. Plots show the frequency of cells in three control *Dpf2<sup>ff</sup>* and three knock-out *Dpf2<sup>ΔΔ</sup>* samples. **(G)** Same as (F), for the myeloid cell markers Gr-1, CD11b and F4-80 and quantification of the frequency of granulocytes (Gr1+ cells) and Macrophages (F4/80+). **(H)** Frequency of the indicated T cell subtypes and NK cells in 14-days old *Dpf2<sup>ff</sup>* and *Dpf2<sup>ΔΔ</sup>* BM mass cytometry samples. CD4+ Naïve T cells correspond to T helper cells (CD4+ CD3e+ CD62L+); CD4+ Memory T cells correspond to CD4+ CD3e+ CD44+ CD62L-; CD4+ T reg cells correspond to CD4+ CD3e+ FOXP3+ and NK cells correspond to CD3e- NK1.1+ cells. **(I)** Frequency of conventional (CD11b+, CD11c+) and plasmacytoid (CD11b-, B220+ CD3e- CD19- NK1.1-) dendritic cells. All bar graph data represent mean  $\pm$  s.e.m. *P* values were calculated using two-tail unpaired Student's t-tests.

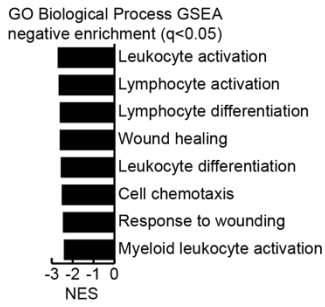




**Supplementary Figure 5. *Dpf2<sup>Δ/Δ</sup>* HSCs have myeloid skewing and impaired homing and engraftment.**

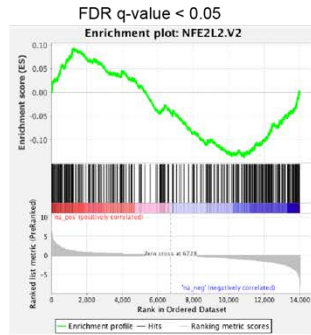
**(A)** Contour plots of abundance of Lin<sup>-</sup> cells (CD4<sup>-</sup> CD8<sup>-</sup> CD19<sup>-</sup> B220<sup>-</sup> TCR<sup>-</sup> Nk<sup>-</sup> Ter119<sup>-</sup>). **(B)** Representative FACS and quantification of the frequency (gated on LK cells) of progenitor populations. CMP, common myeloid progenitors (Lin<sup>-</sup> c-Kit<sup>+</sup> Sca1<sup>-</sup> CD34<sup>+</sup> CD16/32<sup>-</sup>); GMP, granulocyte-macrophage progenitors (Lin<sup>-</sup> c-Kit<sup>+</sup> Sca1<sup>-</sup> CD34<sup>+</sup> CD16/32<sup>+</sup>); MEP, megakaryocyte-erythrocyte progenitors (Lin<sup>-</sup> c-Kit<sup>+</sup> Sca1<sup>-</sup> CD34<sup>-</sup> CD16/32<sup>-</sup>). **(C)** Frequency of CLP (Common lymphoid progenitors; Lin<sup>-</sup> IL7 $\alpha$ <sup>+</sup>; gated on Lin<sup>-</sup>) and lymphoid precursors (Lin<sup>-</sup> c-Kit<sup>-</sup> Sca1<sup>+</sup>). **(D)** Absolute numbers of Lin<sup>-</sup> cells, Lin<sup>-</sup> c-Kit<sup>+</sup> (LK) and Lin<sup>-</sup> c-Kit<sup>+</sup> Sca1<sup>+</sup> (LSK) in BM of end-stage *Dpf2<sup>Δ/Δ</sup>* and age-matched *Dpf2<sup>fl/fl</sup>* mice. **(E)** Absolute numbers of BM MPP, ST-HSC, LT-HSC and progenitor populations. **(F)** Representative image of colonies obtained from Lin<sup>-</sup> cells after 7 days of culture in Methocult M3436. Colonies were harvested and the frequency of cells with the indicated erythroid markers was analyzed. **(G)** Same as (F), for cells cultured in granulocyte-macrophage progenitor Methocult media M3534. The frequency of cells stained with myeloid surface markers Ly6G (Gr-1), CD11b (Mac1) and Ly71(F4/80) was analyzed. **(H)** Frequency of cells with the indicated erythroid surface markers after 7 days of culturing BM Lin<sup>-</sup> cells isolated in liquid media. **(I)** Frequency of myeloid (CD11b<sup>+</sup>) populations collected at the indicated days following a myeloid differentiation protocol (Methods). Cells at day 0 correspond to freshly isolated BM Lin<sup>-</sup> cells. **(J)** Representative FACS and frequency of EdU<sup>+</sup> LT-HSCs (Lin<sup>-</sup> c-Kit<sup>+</sup> Sca1<sup>+</sup> CD150<sup>+</sup>). **(K)** Representative images of Ki67 IHC staining of BM sections. Scale bars represent 100  $\mu$ m. **(L)** Homing analyses of donor (CD45.2<sup>+</sup>) BM cells transplanted into sub-lethally irradiated recipient mice (CD45.1<sup>+</sup>) and analyzed 20 hours after transplant. All bar graph data represent mean  $\pm$  s.e.m. *P* values were calculated using two-tail unpaired Student's t-tests.

A



B

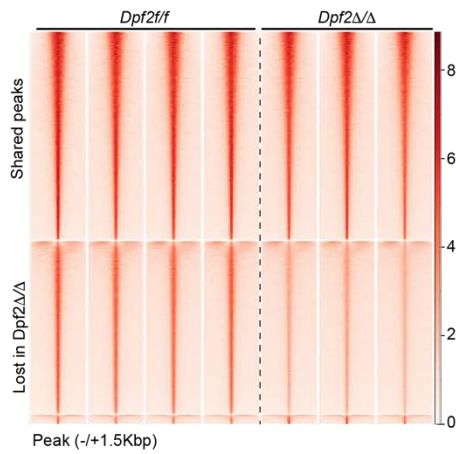
Normalized Enrichment Score (NES): -2.67



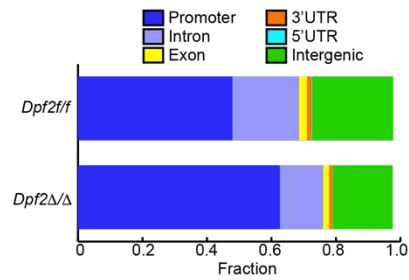
Examples:

*SRXN1* Sulfiredoxin 1  
*NQO1* NAD(P)H quinone dehydrogenase 1  
*GCLM* Glutamate-cysteine ligase modifier subunit  
*GCLC* Glutamate-cysteine ligase catalytic subunit  
*FTH1* Ferritin heavy chain 1  
*TXNRD3* Thioredoxin reductase 3  
*TXNRD1* Thioredoxin reductase 1  
*GSR* Glutathione-disulfide reductase  
*NQO2* N-ribosylidihydro nicotinamide:quinone reductase 2  
*HMOX1* Heme oxygenase 1

C

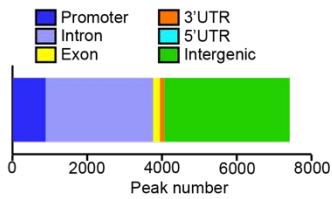


D



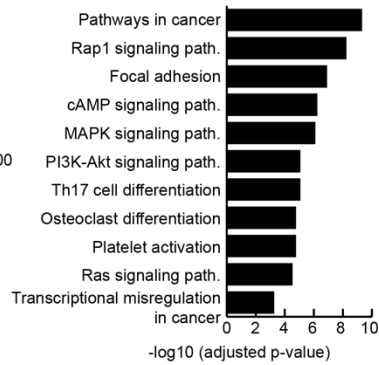
E

ATACseq peaks lost >2FC in *Dpf2ΔΔ*



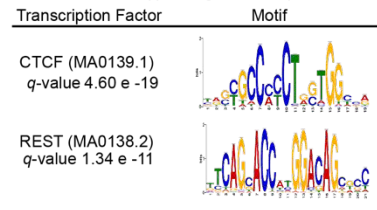
F

3,420 genes (ATACseq peaks lost >2FC)  
KEGG 2019 Mouse



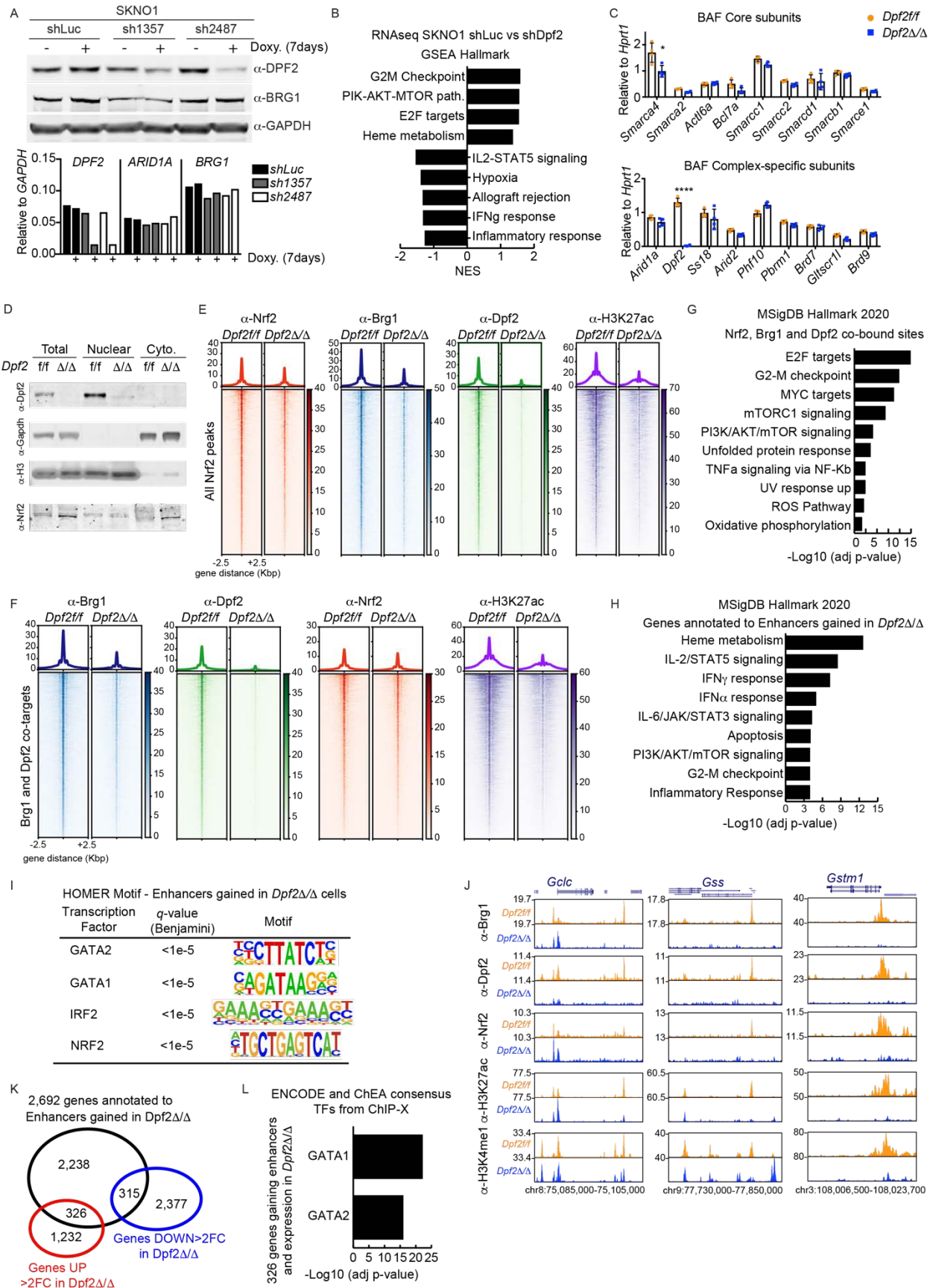
G

ATACseq peaks gained in *Dpf2ΔΔ*



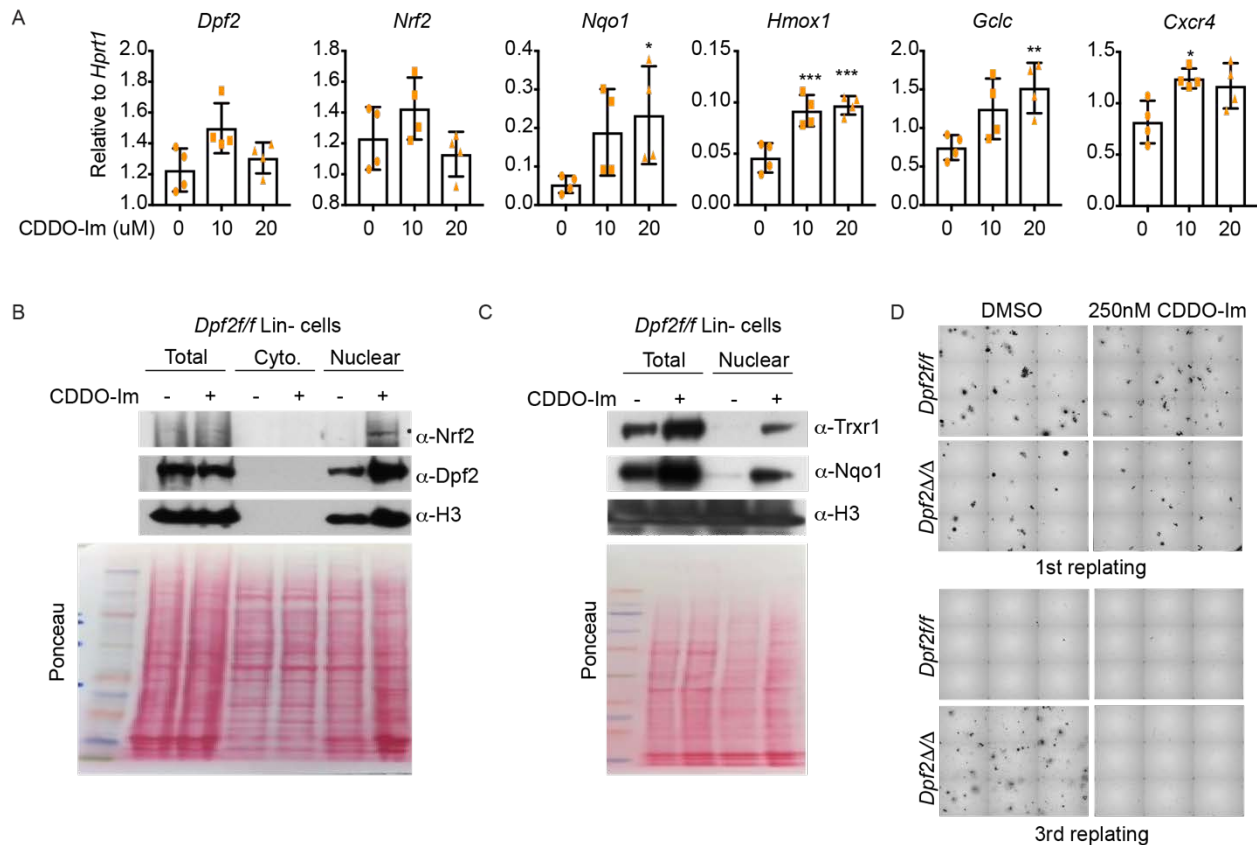
**Supplementary Figure 6. *Dpf2* loss in HSPCs impairs the expression and accessibility of genes controlling differentiation and immune signaling.**

**(A)** GSEA GO Biological Process analysis showing the gene expression pathways deregulated in *Dpf2*<sup>ΔΔ</sup> LK cells compared to *Dpf2*<sup>ff</sup> cells. **(B)** GSEA analysis of genes deregulated in *Dpf2*-deficient LK cells. Relevant examples of genes downregulated in *Dpf2*<sup>ΔΔ</sup> LK cells are listed. **(C)** ATAC-Seq peaks (-/+ 1.5Kbp from peak center) in LK cells from independent mice. **(D)** Genomic distribution of peaks called in *Dpf2*<sup>ff</sup> and *Dpf2*<sup>ΔΔ</sup> LK cells. **(E)** Genomic distribution of peaks with at least 2-fold decrease in ATAC-Seq signal in *Dpf2*<sup>ΔΔ</sup> LK cells compared to *Dpf2*<sup>ff</sup> cells. **(F)** KEGG pathway analyses of 3,420 genes annotated to peaks that lose ATAC-Seq signal intensity at least 2-fold in *Dpf2*<sup>ΔΔ</sup> LK cells compared to *Dpf2*<sup>ff</sup> cells. **(G)** TF motif analysis on ATAC-Seq peaks gained in *Dpf2*<sup>ΔΔ</sup> LK cells.



**Supplementary Figure 7. NRF2, DPF2 and BRG1 co-occupy regulatory regions of genes whose expression is altered following *Dpf2* loss.**

**(A)** Western blot and qRT-PCR showing the expression of *DPF2* and the indicated BAF subunits in SKNO-1 shLuciferase and two independent shRNAs against *DPF2*, induced with doxycycline for 7 days. **(B)** GSEA Hallmark analysis of differentially expressed genes in SKNO-1 *shDPF2* cells compared to shLuciferase control. **(C)** qRT-PCR analysis of the indicated BAF subunits in BM LK cells from 28 days-old mice. Expression is calculated relative to *Hprt1*. **(D)** Subcellular fractionation of Lin<sup>-</sup> cells isolated from *Dpf2<sup>fl/fl</sup>* or *Dpf2<sup>Δ/Δ</sup>* mice. **(E)** Heatmaps of the signal of NRF2, BRG1, DPF2 and H3K27ac at all NRF2 target peaks. **(F)** Heatmaps of the signal of BRG1, DPF2, NRF2 and H3K27ac at BRG1-DPF2 co-bound sites. **(G)** MSigDB Hallmark analyses of 2,812 genes annotated to NRF2, BRG1 and DPF2 co-bound sites. **(H)** MSigDB Hallmark analysis of the 2,692 genes annotated to the 4,527 enhancers gained in *Dpf2<sup>Δ/Δ</sup>* LK cells. **(I)** HOMER motif enrichment analysis on the 4,527 enhancers gained in *Dpf2<sup>Δ/Δ</sup>* LK cells. **(J)** UCSC Genome browser examples of shared NRF2, DPF2 and BRG1 target genes with significantly decreased expression in *Dpf2<sup>Δ/Δ</sup>* LK cells. **(K)** Overlap between 2,692 genes annotated to the 4,527 enhancers gained in *Dpf2<sup>Δ/Δ</sup>* LK cells, and the differentially expressed genes in *Dpf2<sup>Δ/Δ</sup>* compared to *Dpf2<sup>fl/fl</sup>* LK cells ( $q < 0.05$ ; fold change  $> 2$ ). **(L)** ENCODE and ChEA consensus TFs from CHIP-X analysis of the 326 genes that gain enhancers and become upregulated in *Dpf2<sup>Δ/Δ</sup>* LK cells. All bar graph data represent mean  $\pm$  s.e.m. *P* values were calculated using two-tail unpaired Student's t-tests.



**Supplementary Figure 8. Ex vivo treatment with CDDO-Im increases NRF2-target gene expression and impairs the enhanced self-renewal of DPF2-deficient HSPCs.**

**(A)** qRT-PCR analysis of genes in BM LK cells isolated from *Dpf2<sup>ff</sup>* mice treated with vehicle or CDDO-Im for 3 weeks. **(B)** Subcellular fractionation of Lin<sup>-</sup> cells isolated from 1-month old *Dpf2<sup>ff</sup>* mice, treated with vehicle (-) or 300 nM CDDO-Im (+) overnight. Total, cytoplasmic (Cyto.) and nuclear extracts were run, and western blots were probed with the indicated antibodies. Ponceau staining shows comparable total protein levels. **(C)** Subcellular fractionation of *Dpf2<sup>ff</sup>* Lin<sup>-</sup> cells treated with vehicle (-) or 300nM CDDO-Im (+) overnight. **(D)** Representative pictures of CFU assays on the 1<sup>st</sup> or 3<sup>rd</sup> re-plating in vehicle (DMSO) or 250 nM CDDO-Im conditions. All bar graph data represent mean ± s.e.m. *P* values were calculated using one-way ANOVA.